Vortex fluidic mediated one-step fabrication of polyvinyl alcohol hydrogel films with tuning surface morphologies and self-healing property

Javad Tavakoli [1, 2, *], Colin L. Raston [2], Youhong Tang [2, *]

[1] School of Biomedical Engineering, University of Technology Sydney, New South Wales, 2007, Australia

[2] Institute for NanoScale Science and Technology, College of Science and Engineering, Flinders University, South Australia 5042, Australia

* Corresponding authors: Y. Tang (youhong.tang@flinders.edu.au) and J. Tavakoli (javad.tavakoli@uts.edu.au)

Abstract

Previous strategies to control the surface morphology of polyvinyl alcohol (PVA) based hydrogels, including freeze-drying and electrospinning, require a post-treatment process that will affect the final textures and properties. Of particular interest, it is almost impossible to control the surface morphology during the formation of PVA hydrogels using these approaches. The proposed strategy in this study using the novel vortex fluidic device (VFD) technology provides an opportunity for the one-step fabrication of PVA hydrogel films, for the first time. We observed that PVA hydrogel with different surface morphologies including circular patterns containing radial grooves, flat or hollow inside particles with almost irregular shapes, cluster of small sphere-like particles, flower-like patterns, and straight parallel grooves can be readily fabricated using a VFD. Also, we observed that by reducing the concentration of crosslinking agent a self- healed gel with enhanced adhesion strength (60% higher compared to the traditionally-made one) was achieved. Interestingly, the associated self-healing property remained unchanged during 260 s of mechanical test performed with a strain rate of $5\%s^{-1}$. VFD can effectively tune PVA based hydrogel surface morphologies and the associated properties. In particular, the self-healing property of the hydrogels has significantly enhanced.

Keywords

Polyvinyl alcohol, Vortex fluidic device, One-step fabrication, Self-healing, Surface morphology manipulation

1 Introduction

Polyvinyl alcohol (PVA) is a commercially available hydrophilic linear polymer produced via hydrolysis of poly (vinyl acetate), therefore its physicochemical properties including viscosity, adhesion, mechanical strength, and formability depend primarily on the molecular weight of poly (vinyl acetate) and associated degree of hydrolysis [1]. Being chemically inert and stable, PVA is considered safe and its ability to uptake water augments the associated biocompatibility. The degree of hydrolysis determines the swelling capacity of the hydrogel classifying PVA into a low, medium or highly swellable biomaterial [2]. Directly relevant to the degree of hydrolysis, the number of OH group in the PVA molecular structure generally offers crystallization account for physical crosslinking of the hydrogel networks [3]. A highly crystallized PVA hydrogel has low swelling property, making it desirable for specific biomedical and pharmaceutical applications [4-6]. Different studies have shown a notable performance of PVA hydrogel and its composites for wound healing [7], sensors and electrodes [8, 9], tissue engineering [10-12] and biomedical applications [13-15].

Even physically crosslinked PVA hydrogels are highly biocompatibility, a major drawback is the lack of an appropriate strategy to properly tune the associated mechanical and physicochemical properties. Application of freeze-thaw cycles is a solitary approach to enhance the mechanical properties which diversely affect the swelling capacity [16-18]. On the other hand, the final properties of a PVA hydrogel including structural stability, mechanical strength, swelling capacity and rate of drug release can be controlled by using chemical crosslinking agents (i.e. formaldehyde, glutaraldehyde, and ketones) [19-21]. However, the method is toxic, and the biocompatibility of the hydrogel is strongly influenced by the amount of residual crosslinker. Apparently, despite reaching desirable properties via chemical crosslinking, the increase in the level of toxicity alongside with complicated relevant purification strategies compromise the advantages. Recent studies revealed that esterification or formation of hydrogen bonds via the employment of boric acid including borax form an insoluble PVA structure [22, 23]. The method opens new avenues for the fabrication of biocompatible PVA hydrogels with adjustable physicochemical and mechanical properties for different applications [24-27]. Borax has a long history of medical applications having a mean lethal dose exceeding 700 mg/kg in a man with no toxicity reported [28]. Cytotoxicity screening of borax using different cells has shown a non-toxic nature in several studies [23, 24, 29]. Apparently, amongst different methods for crosslinking PVA-based hydrogels, the employment of borax is a facile approach to excessively imposing control over the final

associated properties [30-32]. The approach effectively supports the fabrication of PVA hydrogel composites with different properties ranging from self-adhesion to mechanically strong hydrogels, with a negligible side effect on biomedical properties [33-35].

To the best of our knowledge, independent of the cross-linking method, construction of a bulk PVA hydrogel containing hierarchical architecture or different surface morphology is still challenging. The conventional method to fabricate PVA films is solvent casting that not only involves at least two-steps but also lacks control over surface morphology. Instead, the frequently used methods to control morphology are electrospinning or freeze-drying, which lead to a random fibrous and porous structure, respectively. Both methods require a post crosslinking modification to achieve structural stability and mechanical performance. These post modifications, specifically at a high concentration of crosslinkers, alter the structure and morphology. Of interest, lack of control for surface morphology is a major drawback that affects biomedical applications specifically when cell-surface interaction does matter.

In this study, for the first time, we aim to develop a facile and one-step method to fabricate PVA hydrogels with different surface morphologies that are not attainable by using other fabrication approaches. To investigate this novel concept, a recently developed vortex fluidic device (VFD) was employed (Figure 1a). VFD is a relatively inexpensive research tool for controlling chemical reactivity and selectivity, materials synthesis and probing the structure of self- organized systems, offering a range of benefits over conventional processing [36, 37]. The dynamic thin film within the VFD platform is generated in a rapidly rotating surface, imparting high shear stress and micro-mixing. Typically, quartz or glass tube closed at one end is rapidly rotated at 45^{o} tilt angle, with a finite amount of liquid in the tube, as the confined mode of the VFD, or where liquids are constantly fed into the tube, exiting at the top, as the continuous flow mode of operation. We have successfully employed VFD for a number of diverse applications, including the fabrication of various nanocarbon materials [38, 39], intensified aqueous two-phase separation for protein purification [40], manipulation of polymer networks [41], exfoliation of graphite and boron nitride [42] and protein folding [43]. Of particular interest, we found that the VFD is effective for controlling the size and shape of nanoparticles, for both top-down and bottom-up processing [44].

2 Experimental

2.1. Materials and reagents. Polyvinyl alcohol (PVA) (Mw = 110,000; hydrolysed > 99%) and sodium tetraborate (borax; assay 99%) were purchased from Sigma-Aldrich and used without further purification.

2.2. Sample preparation. PVA (6% w/w) solution was prepared by adding the powder to distilled water at 90 °C with constant stirring (1000 RPM) overnight in a sealed container. Borax solution (100 mM) was prepared by a constant stirring of borax powder in water at 50 °C for 15 min. Both solutions were kept sealed for sample fabrication.

For the one-step fabrication of PVA hydrogels, the VFD tube was filled with 2 mL of borax solution and VFD rotation speeds were set to 1000 - 5000 RPM range. Then using a 5 mL syringe (gauge 18), the PVA solution was injected into the VFD using inlet feed jet (Figure 1b). The formation of hydrogels at different rotation speeds was continued for 5 min before extraction (Figure 1c-top) and PVA hydrogels were dried at room temperature for further assessment. Also, a PVA film was fabricated using the conventional solvent casting method (Figure 1d). Briefly, the PVA solution was cast in a petri dish and placed at room temperature. Upon evaporation of water, the borax solution was added to the petri dish to crosslink the PVA. Also, at the constant rotation speed of 4000 RPM, the effect of time laps and feed jet size was investigated. A high-speed camera (V1212, DANTEC Dynamics) with a 35 mm lens was used to capture transient phenomena at 12,600 fps within the VFD tube upon injection of the PVA solutions. Further, the concentration of the borax solution was reduced to 50 mM to fabricate self-healing PVA gels using both VFD (Figure 1c-bottom) and conventional methods (mixing using a magnet stirrer) and the results were compared for the self-adhesion properties.

2.3. Characterizations. SEM imaging (Inspect F50, FEI Company, USA) was performed to analyze the surface morphology of the PVA films by placing them on an aluminum stub. The PVA films were sputter-coated with platinum at 2 nm thickness. To compare the self-adhesion strength of VFD-driven PVA gels with that of made by the conventional method, a micromechanical machine (CellScale, Canada) was employed. Both VFD-driven and conventionally made PVA hydrogels were cast in a petri dish with a thickness of 2 mm. Then a 10 mm width gel was separated from the center of the petri dish after 10 min and cut into half. Each half was attached to the CellScale actuator securing with a small lab-made gripper while they were not attached. Actuators moved slowly to attach the gels at the cutting edge until the compression force reaching 30 mN. Then, the displacement control tensile test was

executed at the strain rate of 5%s^{-1} for 260 s. During the test, images were captured at the frequency of 1 fps using the CellScale camera. This set up remained unchanged for both VFD-driven and conventionally made PVA hydrogels. Change in adhesion stress was measured as a function of time for 260 s.

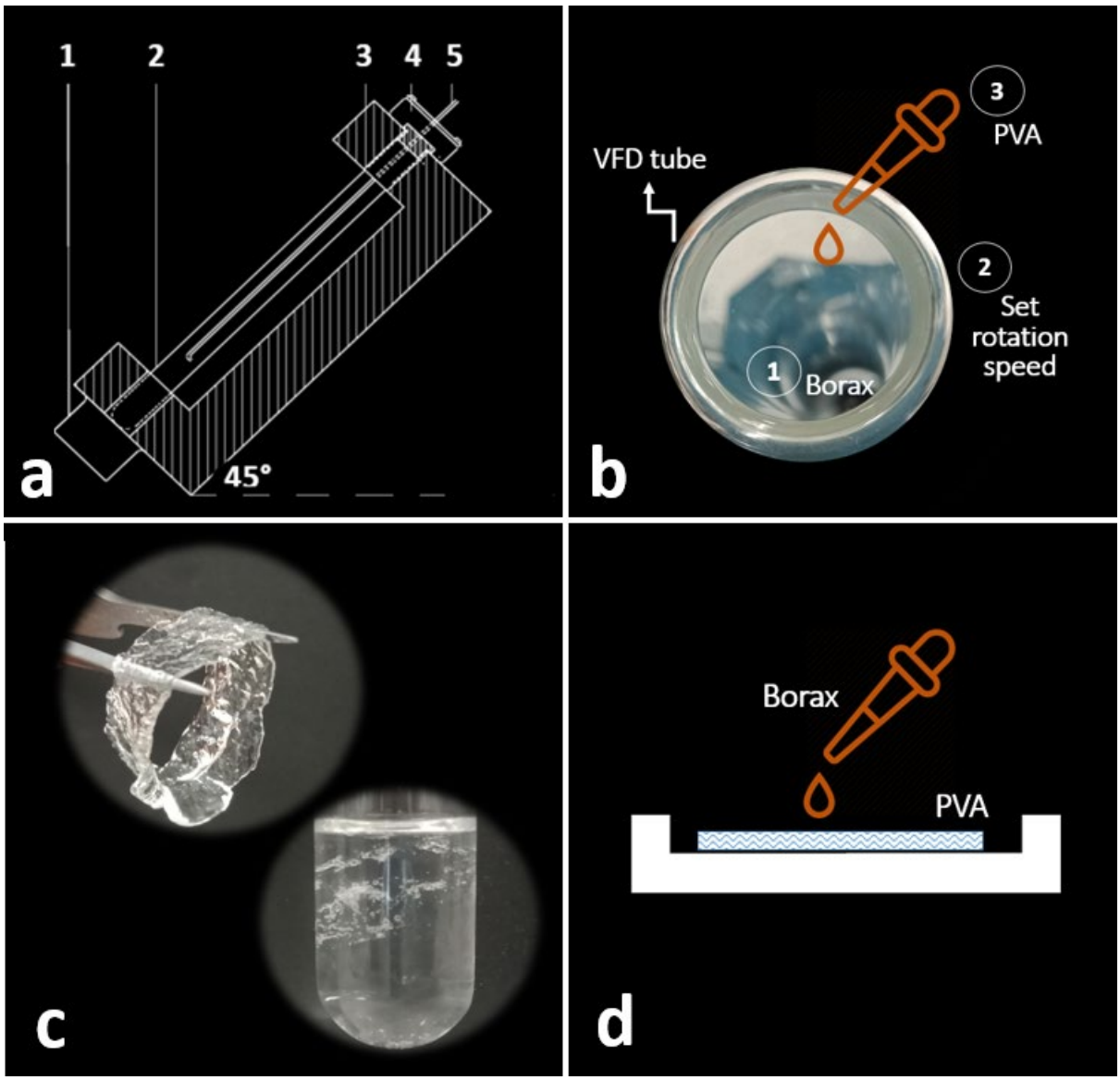

Figure 1. (a) Schematic of a vortex fluidic device (VFD) with highlighting 1, an electric motor, 2, a VFD tube (20 mm diameter), 3, a tube holder, 4, a tube cap and 5, a jet feed inlet, (b) our new approach for the one-step fabrication of PVA hydrogel using VFD to control the surface morphology, (c) the photograph of a PVA hydrogel (top) and self-healing PVA gel (bottom) formulated with different concentrations of borax solution and (d) the conventional approach for fabrication of PVA films.

3 Results and Discussion

3.1 Tuning PVA hydrogel film surface morphology by VFD rotation speeds

Based on the SEM images, no specific pattern was found for the PVA hydrogel films prepared by the conventional method, as expected (Figures 2a and 2b). In contrast, PVA hydrogel films that were prepared using VFD revealed different surface morphologies. At the low rotational speed of 1000 RPM, numerous circular patterns with an approximate diameter of 120- 150 μm, including radial grooves were observed. Interestingly, the grooves were started from the center diverging outward to the perimeter of the circles (Figures 2c and 2d). At the rotational speed of 2000 RPM, PVA films comprised of flat particles ranging 10- 40 μm in size with almost irregular shapes. Our detailed observation at higher magnification revealed distinct regions for the particles including a flat or a hollow central part with slightly elevated edges (Figures 2e and 2f). When the rotation speed was set to 3000 RPM, a cluster of small sphere-like particles with a size of 5- 10 μm irregular distributed across the surface, as shown in Figures 2g and 2h. An increase of rotation speed to 4000 RPM resulted in the formation of a flower-like pattern across the surface of the hydrogel (Figures 2i and 2j) and when the high rotational speed of 5000 RPM was employed, straight parallel grooves with width < 5 μm were formed (Figures 2k and 2l). The forces applied to the PVA solution after injection due to the rotation of the borax solution are likely to be the main cause of these observations. The PVA solution which is injected into the VFD tube experienced different magnitude of the centrifugal force depending on different rotation speeds [44], which is responsible for the formation of different surface morphologies (Figure 2m). Since these observations identified that the formation of different surface morphologies for PVA hydrogel films strongly depends on the magnitude of the applied centrifugal force generated by the rotation of VFD tube, likely, one-step fabrication of PVA hydrogel films with different surface texture are reproducible. Therefore, the proposed method opens new avenues in the preparation of hydrogel films with customized surface texture.

We found that by precisely varying the rotation speed of the VFD tube, PVA hydrogel films with different surface morphologies were readily fabricated. Our observations based on SEM images revealed that VDF plays an important role to develop a new strategy for a one-step fabrication of PVA hydrogel films with different surface architectures. This unique approach is likely to be readily extended for the fabrication of other natural-based hydrogels that are crosslinked by borax or ionic solutions [23, 45].

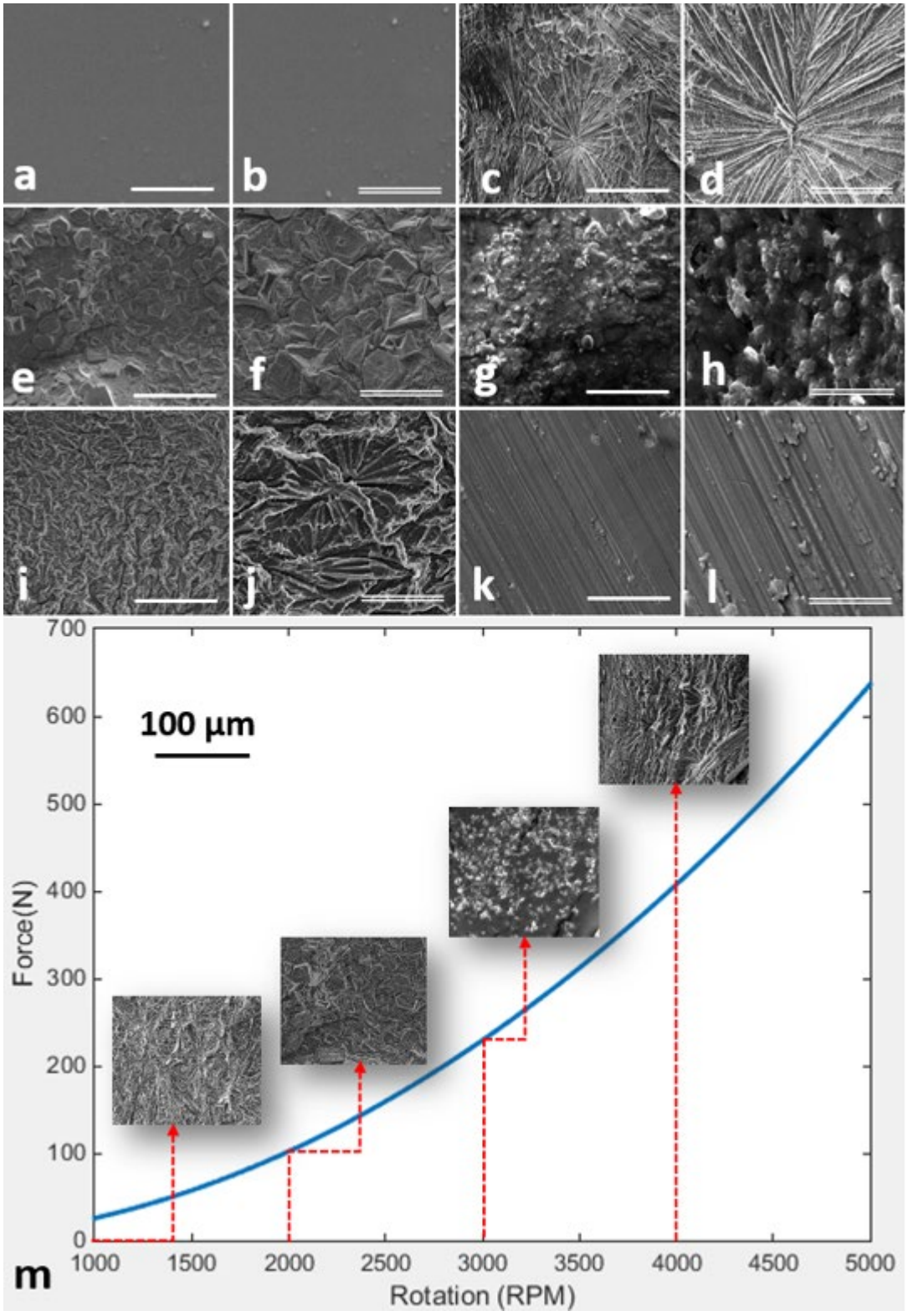

Figure 2. SEM images of the surface of PVA hydrogel films fabricated using (a) and (b) the traditional method compared to the VFD-driven method at different rotation speeds of (c) and (d) 1000, (e) and (f) 2000, (g) and (h) 3000, (i) and (j) 4000 and (k) and (l) 5000 RPM. Scale bars representing two magnifications of 200 and 50 µm. (m) Change in the centrifugal force

experienced by PVA film at different rotation speeds which resulted in the formation of different surface morphologies (insets).

3.2. VFD jet feed inlet effect on PVA hydrogel surface morphology

In further investigation, the PVA solution was injected into the VFD tube rotating at 4000 RPM using jet feed inlets with two different diameters of 1 mm and a gauge 18 syringe, as shown in insets of Figures 3(a) and 3(b). Interestingly, we found a significant change for the surface morphology of the PVA films using different jet feed inlets with two different diameters. The employment of two different jet feeds resulted in the formation of a flower-like structure on the surface of the PVA hydrogel. However, when a needle-like jet feed inlet was used those structures were smaller with elevated edges and smooth inner regions. A bigger flower-like structure containing leaf-like veins was observed for the bigger diameter of jet feed. When a gauge 18 syringe jet feed has recruited the surface of regions excluding the flowers seemed to pack with small spherical structures.

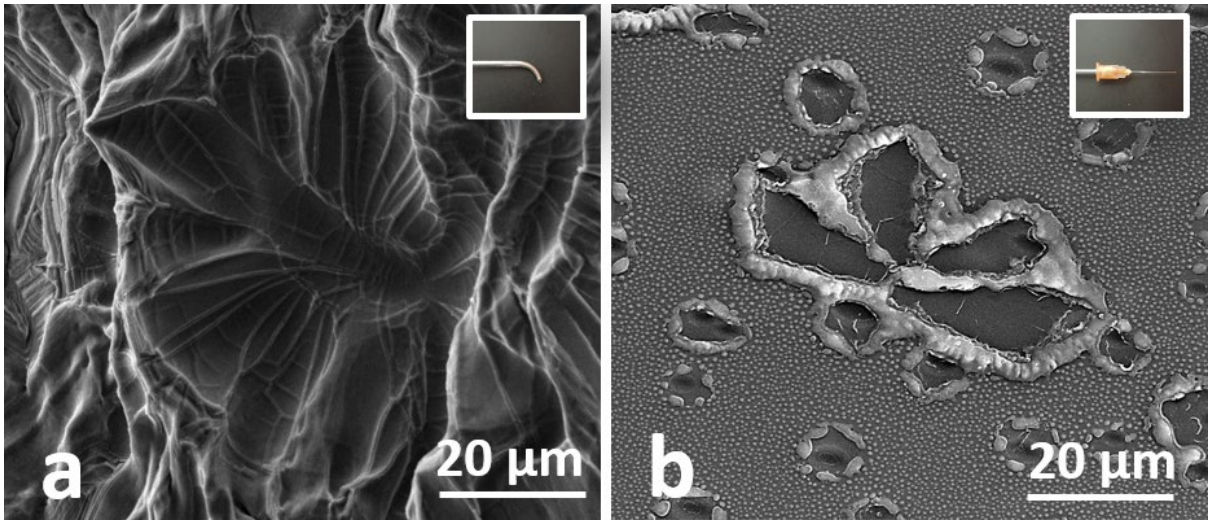

Figure 3- SEM images of the surface of PVA hydrogels fabricated in a rotating VFD tube at 4000 RPM using (a) 1 mm diameter and (b) a gauge 18 syringe jet feeds. The inset images showed two different types of jet feeds.

3.3. Mechanism understanding of the formation of the VFD-driven PVA hydrogel film

To obtain a deeper insight into understanding the mechanism of PVA hydrogel film formation using VFD, different strategies were investigated. Firstly, images that were captured during the injection of PVA solution into the VFD tube using a high-speed camera revealed that PVA droplets are unlikely to turn into or form particles before attaching to the surface of the tube (Supplementary movie 1). To further investigate this observation, SEM images were captured from both top and back layers of the PVA hydrogel films at different rotation speeds (1000-4000 RPM) as shown in Figures 4a-4c. We found that the back layer of the PVA hydrogel films was smooth surface without any specific pattern or morphology confirming our observation using a high-speed camera. Secondly, at the constant rotation speed of 4000 RPM, the effect of time-lapse on the formation of PVA hydrogel films was explored. In a series of individual experiments, the PVA solution was injected into the borax solution using a 1 mm jet feed inlet, while the rotation of the VFD tube was set to 4000 RPM. At different time points of 1, 2 and 4 min the PVA hydrogel films were extracted and SEM images were captured. As shown in Figures 4d-4f, the surface of the hydrogel was subjected to change at different time points. Change in the morphology of the PVA hydrogel films initiates at the surface which is the first region being exposed to the borax solution. It is believed that following the injection of PVA solution into the borax solution in the rotating VFD tube, diffusion of borax into the flattened PVA solution is the main reason for the formation of the PVA hydrogel film. Since the outer region of the flattened PVA solution is the first region that is exposed to the crosslinking agent, it is likely that a core-shell PVA hydrogel film forms with a PVA solution enclosed inside a soft crosslinked shell. Later, the progress of the diffusion process resulted in crosslinking the bulk of the PVA hydrogel leading to the formation of a hydrogel film with different morphologies. At the beginning of the crosslinking process, the crosslinked shell (outer surface) is soft and therefore the distribution of the centrifugal force results in the formation of texture on the surface of the PVA hydrogel film. Since the centrifugal force is proportional to the rotating speed, any specific rotation speed has its impact leading to the formation of unique surface morphology.

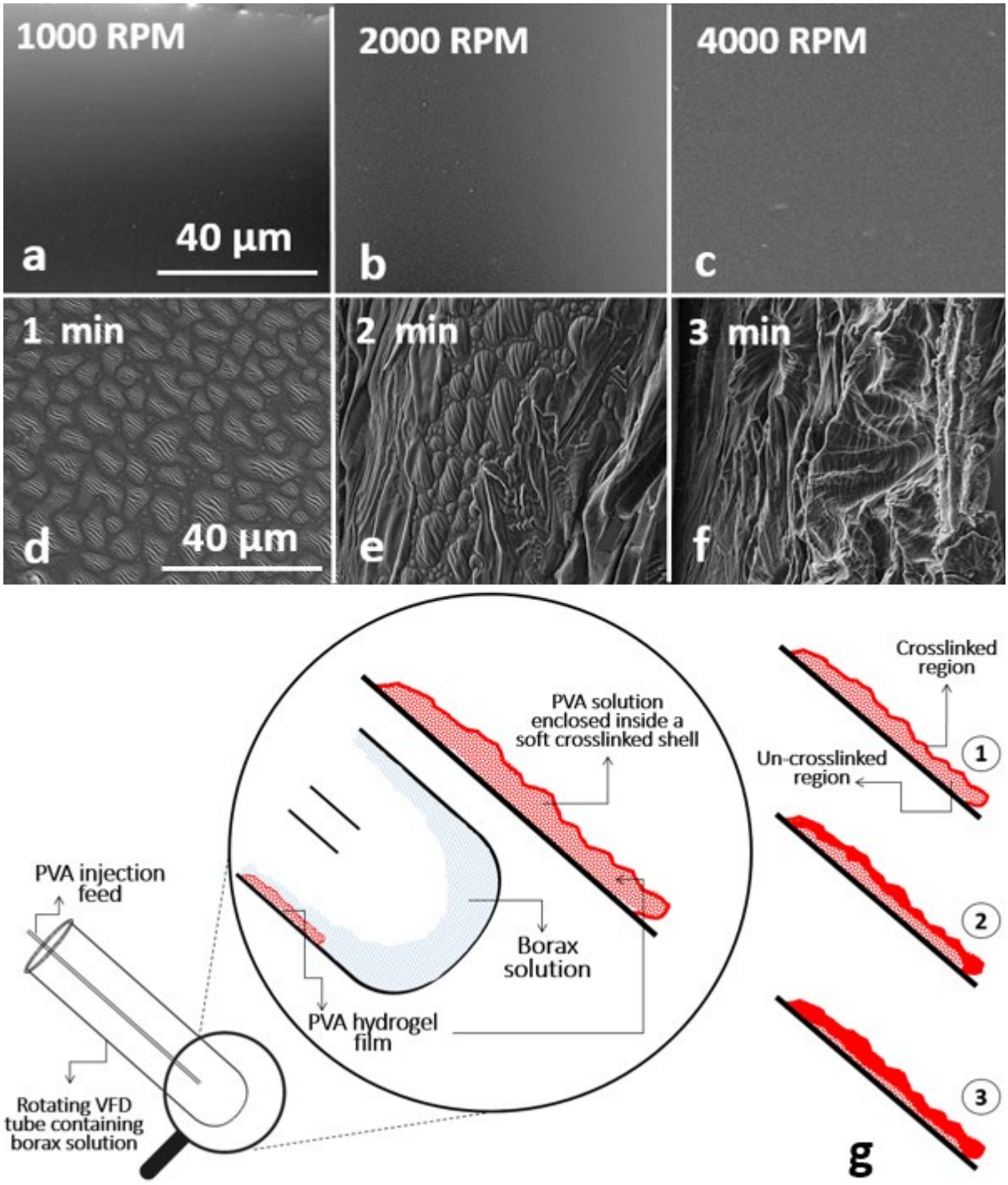

Figure 4. (a-c) The SEM images of PVA hydrogel films captured from their back layer at different rotation speeds. (d-f) The SEM images of the surface of the PVA hydrogel films that were crosslinked at different time points of 1, 2 and 4 min at rotation speed = 4000 RPM. (g) A schematic drawing to illustrate the mechanism of PVA hydrogel formation using VFD. A magnified cross-section of the VFD tube after injection of PVA solution into the rotating borax solution revealing the formation of a core-shell structure as the outer surface of the PVA

solution is in contact with the borax solution first. The diffusion of borax as a function of time (1-3) into the core-shell PVA film results in the formation of PVA film hydrogel.

3.4. Significantly enhanced self-healing properties of PVA hydrogels under VFD formation

We found that a decrease in the concentration of the crosslinking agent, borax in this study led to the preparation of a PVA-based solution with strong self-healing property. Our observation confirmed that at 4000 RPM rotation of the VFD tube, the use of 50 mM borax resulted in the formation of a highly extensible PVA hydrogel with improved self-adhesion property (Supplementary movies 2-5). In contrast, traditionally prepared PVA hydrogel (mixing of borax and PVA solution without the employment of VDF) suffered both strong self-adhesion property and low extensibility. By quantifying the self-adhesion stress at the cutting edge of the gel, our experimental results revealed that detachment occurred at 40% strain for the traditionally prepared PVA hydrogel, which was significantly lower than that of the VFD-driven PVA hydrogel prepared at 4000 RPM. The detachment between cutting edges of VFD-driven PVA hydrogel wasn't seen even at a 250% strain (Figure 5). Interestingly, we found that after application of $5\%s^{-1}$ strain for 260 s, VFD-driven PVA hydrogel experienced 5.6 mN/mm^2 adhesion stress while still was attached. The adhesion stress for traditionally prepared PVA hydrogel was approximately 3.5 mN/mm^2 at the breaking point that occurred after the application of strain for 120 min. A 60% improvement in adhesion strength was seen when VFD was employed for the fabrication of PVA-based self-healing hydrogel, compared to the hydrogels that were prepared using a traditional approach. This observation can be explained based on the formation of a more homogeneous structure when the VFD was employed. The precise mixing of PVA and borax solution which is readily achievable by using the VFD led to a better spatial distribution of borax molecules within the PVA chains. This, in turn, resulted in the formation of a more uniform structure that isn't identical to that of PVA hydrogel prepared by the traditional method. In fact, the propagation of borax molecules within the PVA chains is not uniform when a traditional method was recruited and it is more likely this simple mixing led to the agglomeration of borax. Therefore at the micro-level, a more heterogeneous structure consisting of aggregated borax molecules was formed that is responsible for the lower self-healing properties (Figure 5h).

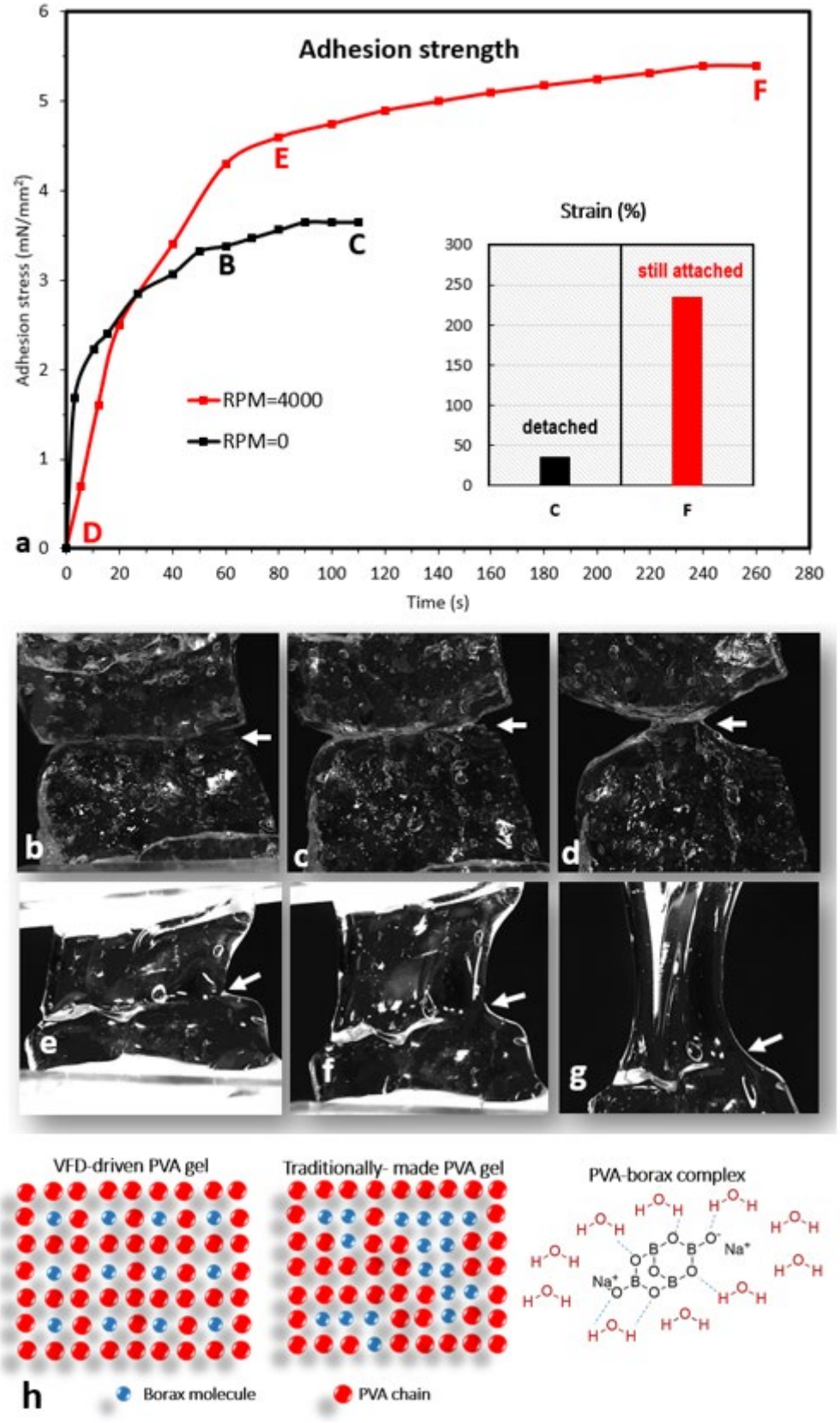

Figure 5. (a) Comparing the adhesion strength and the extensibility of PVA- based hydrogels prepared traditionally and using a VDF. The magnified images (×4) were captured during the

measurement of the self-adhesion property of (b-d) traditionally prepared and (e-g) VFD-driven PVA-based hydrogels. White arrows identify the cutting edges during the test. To execute the experiment, the cutting edges were re-attached before extension as explained before. (h) Schematic drawing and the chemical structure of PVA-borax complex, indicating a heterogeneous structure for the VFD-driven PVA gel compared to a heterogeneous structure including aggregation of borax molecules for the traditionally-made PVA gel.

The associated movies (Supplementary movies 6-7) indicating the self-healing property of the PVA-based hydrogels during the measurement of adhesion strength.

4 Conclusions

The one-step preparation of PVA- based hydrogel films under thin film formation is reported in this student which provides a new strategy to control the surface morphologies during the preparation of hydrogels. By changing both rotation speed and crosslinking density during the preparation of hydrogels, the texture of the surface, as well as the self-healing property, can be significantly tunned with the higher speed increasing extensibility and self-adhesion strength significantly. The direct control of surface morphology, as an advantage of employment of VFD, opens new opportunities for biological and material studies.

Acknowledgments

J. T. and Y. T. acknowledges an International Research Grant (International Laboratory for Health Technologies) of South Australia and Australia-China Science and Research Fund-Joint Research Centre on Personal Health Technologies for support. C. R. thanks the support from the Australian Research Council. The expertise, equipment, and support provided by Microscopy Australia and the Australian National Fabrication Facility at the South Australian nodes under the National Collaborative Research Infrastructure Strategy are acknowledged.

Conflict of interest

The authors declare that they have no conflict of interest.

Supplementary information

Supporting movies are available online

References

[1] Cascone S, Lamberti G. Hydrogel-based commercial products for biomedical applications: A review. *International journal of pharmaceutics*, 2020, 573(118803

[2] Tavakoli J, Zhang H-p, Tang BZ, et al. Aggregation-induced emission lights up the swelling process: A new technique for swelling characterisation of hydrogels. *Materials Chemistry Frontiers*, 2019, 3(4): 664-667

[3] Tavakoli J, Gascooke J, Xie N, et al. Enlightening freeze–thaw process of physically cross-linked poly(vinyl alcohol) hydrogels by aggregation-induced emission fluorogens. *ACS Applied Polymer Materials*, 2019, 1(6): 1390-1398

[4] Tavakoli J, Tang Y. Hydrogel based sensors for biomedical applications: An updated review. *Polymers (Basel)*, 2017, 9(8):

[5] Jia R, Li L, Ai Y, et al. Self-healable wire-shaped supercapacitors with two twisted nico2o4 coated polyvinyl alcohol hydrogel fibers. *Science China Materials*, 2018, 61(2): 254-262

[6] Zhang X, Xia L-Y, Chen X, et al. Hydrogel-based phototherapy for fighting cancer and bacterial infection. *Science China Materials*, 2017, 60(6): 487-503

[7] Tavakoli J, Mirzaei S, Tang Y. Cost-effective double-layer hydrogel composites for wound dressing applications. *Polymers (Basel)*, 2018, 10(3):

[8] Yan W, Chen Q, Meng X, et al. Multicycle photocatalytic reduction of cr(vi) over transparent pva/tio2 nanocomposite films under visible light. *Science China Materials*, 2017, 60(5): 449-460

[9] Li S-K, Mao L-B, Gao H-L, et al. Bio-inspired clay nanosheets/polymer matrix/mineral nanofibers ternary composite films with optimal balance of strength and toughness. *Science China Materials*, 2017, 60(10): 909-917

[10] Zhong L, Qu Y, Shi K, et al. Biomineralized polymer matrix composites for bone tissue repair: A review. *Science China Chemistry*, 2018, 61(12): 1553-1567

[11] Baker MI, Walsh SP, Schwartz Z, et al. A review of polyvinyl alcohol and its uses in cartilage and orthopedic applications. *Journal of Biomedical Materials Research Part B: Applied Biomaterials*, 2012, 100(5): 1451-1457

[12] Slaughter BV, Khurshid SS, Fisher OZ, et al. Hydrogels in regenerative medicine. *Advanced materials*, 2009, 21(32‐33): 3307-3329

[13] Costa-Júnior ES, Barbosa-Stancioli EF, Mansur AAP, et al. Preparation and characterization of chitosan/poly (vinyl alcohol) chemically crosslinked blends for biomedical applications. *Carbohydrate Polymers*, 2009, 76(3): 472-481

[14] Dehbari N, Tavakoli J, Zhao J, et al. In situ formed internal water channels improving water swelling and mechanical properties of water swellable rubber composites. *Journal of Applied Polymer Science*, 2017, 134(9):

[15] Liu J, Ye J, Pan F, et al. Solid-state yet flexible supercapacitors made by inkjet-printing hybrid ink of carbon quantum dots/graphene oxide platelets on paper. *Science China Materials*, 2019, 62(4): 545-554

[16] Chee BS, de Lima GG, Devine DM, et al. Investigation of the effects of orientation on freeze/thawed polyvinyl alcohol hydrogel properties. *Materials Today Communications*, 2018, 17(82-93

[17] Peppas NA, Scott JE. Controlled release from poly (vinyl alcohol) gels prepared by freezing-thawing processes. *Journal of controlled release*, 1992, 18(2): 95-100

[18] Hassan CM, Peppas NA. Cellular pva hydrogels produced by freeze/thawing. *Journal of Applied Polymer Science*, 2000, 76(14): 2075-2079

[19] Mansur HS, Sadahira CM, Souza AN, et al. Ftir spectroscopy characterization of poly (vinyl alcohol) hydrogel with different hydrolysis degree and chemically crosslinked with glutaraldehyde. *Materials Science and Engineering: C*, 2008, 28(4): 539-548

[20] Ossipov DA, Hilborn J. Poly (vinyl alcohol)-based hydrogels formed by “click chemistry”. *Macromolecules*, 2006, 39(5): 1709-1718
[21] Schmedlen RH, Masters KS, West JL. Photocrosslinkable polyvinyl alcohol hydrogels that can be modified with cell adhesion peptides for use in tissue engineering. *Biomaterials*, 2002, 23(22): 4325-4332
[22] Han J, Lei T, Wu Q. Facile preparation of mouldable polyvinyl alcohol-borax hydrogels reinforced by well-dispersed cellulose nanoparticles: Physical, viscoelastic and mechanical properties. *Cellulose*, 2013, 20(6): 2947-2958
[23] Tavakoli J. Physico-mechanical, morphological and biomedical properties of a novel natural wound dressing material. *J Mech Behav Biomed Mater*, 2017, 65(373-382
[24] Tavakoli J, Tang Y. Honey/pva hybrid wound dressings with controlled release of antibiotics: Structural, physico-mechanical and in-vitro biomedical studies. *Mater Sci Eng C Mater Biol Appl*, 2017, 77(318-325
[25] Han J, Lei T, Wu Q. High-water-content mouldable polyvinyl alcohol-borax hydrogels reinforced by well-dispersed cellulose nanoparticles: Dynamic rheological properties and hydrogel formation mechanism. *Carbohydrate polymers*, 2014, 102(306-316
[26] Spoljaric S, Salminen A, Luong ND, et al. Stable, self-healing hydrogels from nanofibrillated cellulose, poly (vinyl alcohol) and borax via reversible crosslinking. *European Polymer Journal*, 2014, 56(105-117
[27] Yang N, Qi P, Ren J, et al. Polyvinyl alcohol/silk fibroin/borax hydrogel ionotronics: A highly stretchable, self-healable, and biocompatible sensing platform. *ACS applied materials & interfaces*, 2019,
[28] Balakrishnan B, Jayakrishnan A. Self-cross-linking biopolymers as injectable in situ forming biodegradable scaffolds. *Biomaterials*, 2005, 26(18): 3941-3951
[29] Yang N, Qi P, Ren J, et al. Polyvinyl alcohol/silk fibroin/borax hydrogel ionotronics: A highly stretchable, self-healable, and biocompatible sensing platform. *ACS Applied Materials & Interfaces*, 2019, 11(26): 23632-23638
[30] Jian M, Wang C, Wang Q, et al. Advanced carbon materials for flexible and wearable sensors. *Science China Materials*, 2017, 60(11): 1026-1062
[31] Ochiai H, Fukushima S, Fujikawa M, et al. Mechanical and thermal properties of poly(vinyl alcohol) crosslinked by borax. *Polymer Journal*, 1976, 8(1): 131-133
[32] Lu B, Lin F, Jiang X, et al. One-pot assembly of microfibrillated cellulose reinforced pva–borax hydrogels with self-healing and ph-responsive properties. *ACS Sustainable Chemistry & Engineering*, 2016, 5(1): 948-956
[33] Lawrence MB, Joseph J, Phondekar K, et al. Dc conductivity behaviour of poly (vinyl alcohol)-based ferrogels: Role of borax and carbonyl iron. *Polymer Bulletin*, 2019, 1-15
[34] Ge W, Cao S, Shen F, et al. Rapid self-healing, stretchable, moldable, antioxidant and antibacterial tannic acid-cellulose nanofibril composite hydrogels. *Carbohydrate polymers*, 2019, 224(115147
[35] Jing Z, Xu A, Liang Y-Q, et al. Biodegradable poly (acrylic acid-co-acrylamide)/poly (vinyl alcohol) double network hydrogels with tunable mechanics and high self-healing performance. *Polymers*, 2019, 11(6): 952
[36] Britton J, Stubbs KA, Weiss GA, et al. Vortex fluidic chemical transformations. *Chemistry–A European Journal*, 2017, 23(54): 13270-13278
[37] Yasmin L, Chen X, Stubbs KA, et al. Optimising a vortex fluidic device for controlling chemical reactivity and selectivity. *Scientific reports*, 2013, 3(2282
[38] Vimalanathan K, Gascooke JR, Suarez-Martinez I, et al. Fluid dynamic lateral slicing of high tensile strength carbon nanotubes. *Scientific reports*, 2016, 6(22865
[39] Luo X, Al-Antaki AHM, Vimalanathan K, et al. Laser irradiated vortex fluidic mediated synthesis of luminescent carbon nanodots under continuous flow. *Reaction Chemistry & Engineering*, 2018, 3(2): 164-170

[40] Luo X, Smith P, Raston C, et al. Vortex fluidic device-intensified aqueous two phase extraction of c-phycocyanin from spirulina maxima. *ACS Sustainable Chemistry & Engineering*, 2016, 4(7): 3905-3911
[41] Luo X, Al‐Antaki AHM, Pye S, et al. High‐shear‐imparted tunable fluorescence in polyethylenimines. *ChemPhotoChem*, 2018, 2(4): 343-348
[42] Chen X, Dobson JF, Raston CL. Vortex fluidic exfoliation of graphite and boron nitride. *Chemical Communications*, 2012, 48(31): 3703-3705
[43] Yuan TZ, Ormonde CF, Kudlacek ST, et al. Shear‐stress‐mediated refolding of proteins from aggregates and inclusion bodies. *ChemBioChem*, 2015, 16(3): 393-396
[44] Tavakoli J, Pye S, Reza AHMM, et al. Tuning aggregation-induced emission nanoparticle properties under thin film formation. *Materials Chemistry Frontiers*, 2020,
[45] Tavakoli J, Laisak E, Gao M, et al. Aiegen quantitatively monitoring the release of ca2+ during swelling and degradation process in alginate hydrogels. *Materials Science and Engineering: C*, 2019, 104(109951